RSC Advances

PAPER

View Article Online
View Journal | View Issue

Cite this: *RSC Adv.*, 2019, **9**, 37331

Four rare structurally characterized hetero-pentanuclear [Zn_4Ln] bis(salamo)-type complexes: syntheses, crystal structures and spectroscopic properties†

Lu-Mei Pu,*[a] Lan Wang,[b] Xiao-Yan Li,[b] Yin-Xia Sun,[b] Quan-Peng Kang,[b] Hai-Tao Long,[a] Wei-Bing Xu [a] and Wen-Kui Dong *[b]

Received 15th September 2019
Accepted 6th November 2019

DOI: 10.1039/c9ra07423f

rsc.li/rsc-advances

Four new hetero-pentanuclear 3d–4f complexes [$Zn_4(L)_2La(NO_3)_2(OEt)(H_2O)$] (**1**), [$Zn_4(L)_2Ce(NO_3)_2$-(OMe)(MeOH)] (**2**), [$Zn_4(L)_2Pr(NO_3)_2(OEt)(EtOH)$] (**3**) and [$Zn_4(L)_2Nd(NO_3)_2(OMe)(MeOH)$] (**4**) were synthesized by the reactions of a newly synthesized octadentate bis(salamo)-based tetraoxime ligand (H_4L) with $Zn(OAc)_2\cdot 2H_2O$ and $Ln(NO_3)_3\cdot 6H_2O$ (Ln = La, Ce, Pr and Nd), respectively, and characterized *via* elemental analyses, FT-IR, UV-Vis spectroscopy and single crystal X-ray crystallography. The X-ray crystallographic investigation revealed that all Zn^{II} ions were located in N_2O_3 coordination spheres, and possessed a trigonal bipyramid coordination environment. The Ln^{III} ion lay in an O_8 coordination sphere, and adopted a distorted square antiprismatic coordination environment. Furthermore, supramolecular interactions and fluorescence properties were investigated.

1 Introduction

Salen-type ligands and their analogues are very versatile chelating ligands in inorganic and organometallic chemistry.[1] Their complexes have considerable intrinsic value due to their wide applications in electrochemistry,[2] building supramolecular structures,[3] catalysis fields,[4] magnetism,[5] biological fields[6] and so forth.

In recent years, a preferable class of salen-type compounds (salamo: (R–CH=N–O–$(CH_2)_n$–O–N=CH–R)) has been reported,[7] and the large electronegativity of O atoms is expected to lead to different and novel structures and properties of the resulting complexes. The 3d–4f complexes have attracted much attention due to the visible and near-infrared luminescence produced by lanthanide f–f transitions.[8] Luminescence applications of lanthanides are a consequence of their narrow emission bands, large Stokes shifts, negligible environmental influences and relatively long luminescence lifetimes. However, 3d–4f complexes with salamo-like ligands have been rarely reported.[9]

Herein, a series of rare heteropentanuclear [Zn_4Ln] (Ln = La, Ce, Pr and Nd) complexes containing octadentate bis(salamo)-based tetraoxime ligand H_4L were synthesized and structurally characterized. Meanwhile, the luminescence properties of complexes **1–4** were studied.

2 Experimental

2.1. Materials and methods

1,2-Dimethoxybenzene, 1,2-dibromoethane, TMEDA, *n*-butyllithium, boron tribromide and 2-hydroxy-1-naphthaldehyde (99%) were purchased from Alfa Aesar and used without further purification. Other reagents and solvents were analytical grade reagents from Tianjin Chemical Reagent Factory.

Elemental analyses for carbon, hydrogen and nitrogen were obtained using a GmbH VariuoEL V3.00 automatic elemental analysis instrument (Berlin, Germany). La^{III}, Ce^{III}, Pr^{III} and Nd^{III} were gained using an IRIS ER/S-WP-1 ICP atomic emission spectrometer (Berlin, Germany). Melting points were obtained *via* a microscopic melting point apparatus made by Beijing Taike Instrument Company Limited. IR spectra (4000–400 cm^{-1}) were determined *via* a Vertex 70 FT-IR spectrophotometer (Bruker, Billerica, MA, USA), with samples prepared as KBr pellets. UV-Vis absorption spectra were determined using a Shimadzu UV-3900 spectrometer (Shimadzu, Japan). ^1H NMR spectra were determined *via* German Bruker AVANCE DRX-400/600 spectroscopy. X-ray single crystal structure determinations for complexes **1**, **2**, **3** and **4** were carried out on a Bruker APEX-II CCD diffractometer. Fluorescence spectra were recorded on an F-7000 FL

[a]*College of Science, Gansu Agricultural University, Lanzhou, Gansu 730070, P. R. China. E-mail: pulm@gsau.edu.cn*

[b]*College of Chemical and Biological Engineering, Lanzhou Jiaotong University, Lanzhou, Gansu, 730070, P. R. China. E-mail: dongwk@126.com*

† Electronic supplementary information (ESI) available. CCDC 1894560, 1894557, 1894559 and 1894558 for complexes **1–4**. For ESI and crystallographic data in CIF or other electronic format see DOI: 10.1039/c9ra07423f

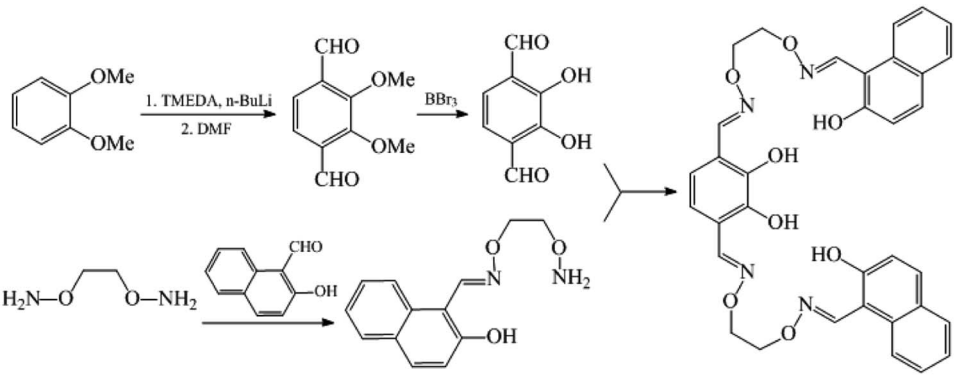

Scheme 1 Synthetic route to H_4L.

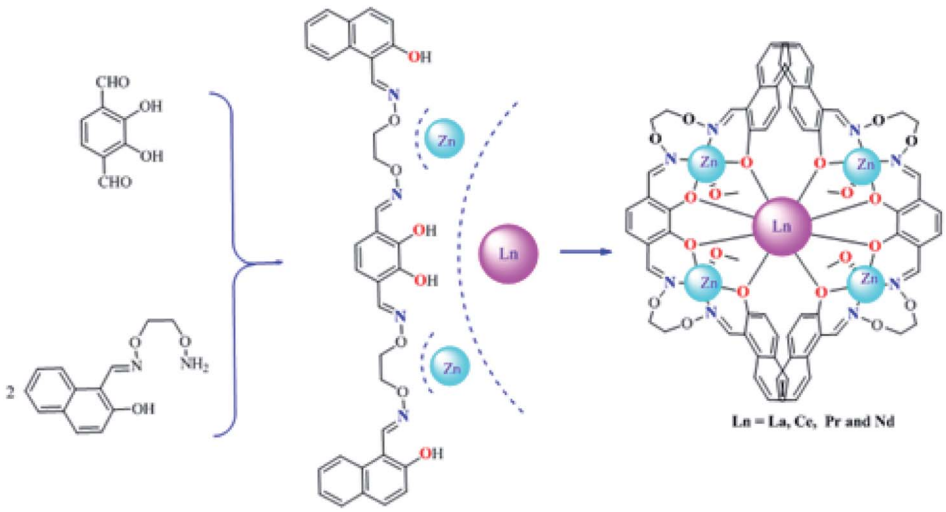

Scheme 2 Synthetic routes to H_4L and its complexes **1–4**.

spectrophotometer. Near infrared (NIR) spectra were determined through PTI QM_4 spectrofluorometer with a PTI QM_4 Near infrared InGaAs detector.

2.2. Synthesis of the H_4L

The reaction steps of the ligand (H_4L) can be seen from Scheme 1. 1,2-Bis(aminooxy)ethane, 2,3-dihydroxybenzene-1,4-dicarbal-

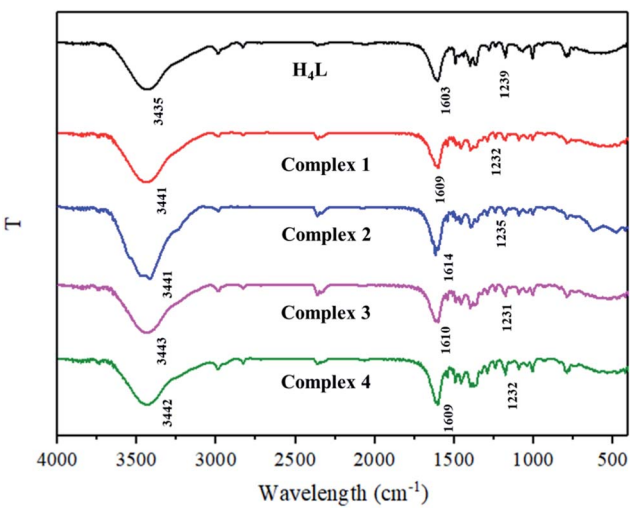

Fig. 1 IR spectra of H_4L and its corresponding complexes **1–4**.

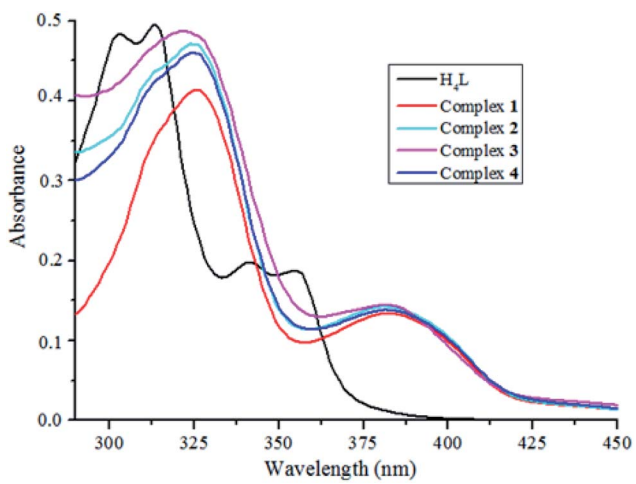

Fig. 2 UV-Vis spectra of the free ligand H_4L and its complexes **1–4**.

Table 1 Crystal data and the structure refinements for complexes 1–4

Complex	1	2	3	4
Empirical formula	$C_{70}H_{59}LaZn_4N_{10}O_{24}$	$C_{70}H_{59}CeZn_4N_{10}O_{24}$	$C_{72}H_{63}PrZn_4N_{10}O_{24}$	$C_{70}H_{59}NdZn_4N_{10}O_{24}$
Formula weight	1824.66	1824.86	1854.71	1829.99
T (K)	296(2)	173(2)	173(2)	173(2)
Wavelength (Å)	0.71073	0.71073	0.71073	0.71073
Crystal system	Monoclinic	Monoclinic	Monoclinic	Monoclinic
Space group	$C2/c$	$C2/c$	$C2/c$	$C2/c$
a (Å)	23.8927(11)	16.9226(7)	16.7809(7)	16.9226(7)
b (Å)	15.5212(7)	23.3361(10)	23.4499(7)	23.3361(10)
c (Å)	45.813(2)	24.4208(13)	24.1484(11)	24.4208(13)
α (°)	90	90	90	90
β (°)	97.7300(10)	109.4290(10)	108.736(5)	109.4290(10)
γ (°)	90	90	90	90
V (Å^3)	16 835.2(13)	9094.8(7)	8999.1(7)	9094.8(7)
Z	8	4	4	4
$D_{calc.}$ (g cm^{-3})	1.440	1.333	1.369	1.336
Absorption coefficient (mm^{-1})	1.694	1.599	1.653	1.669
F (000)	7344	3672	3744	3684
Crystal size (mm)	0.270 × 0.250 × 0.220	0.220 × 0.190 × 0.160	0.220 × 0.200 × 0.180	0.220 × 0.190 × 0.160
θ Range (°)	2.044–25.010	2.485–25.008	1.548–26.000	2.485–25.008
Index ranges	$-25 \le h \le 28$ $-18 \le k \le 18$ $-51 \le l \le 54$	$-20 \le h \le 20$ $-22 \le k \le 27$ $-29 \le l \le 29$	$-20 \le h \le 20$ $-27 \le k \le 28$ $-29 \le l \le 29$	$-20 \le h \le 17$ $-27 \le k \le 27$ $-29 \le l \le 28$
Reflections collected/unique	59 539/14 818 [$R_{int} = 0.0347$]	32 276/7999 [$R_{int} = 0.0371$]	19 902/8832 [$R_{int} = 0.0179$]	32 970/8002 [$R_{int} = 0.0391$]
Completeness to θ	99.8% ($\theta = 25.010$)	99.8% ($\theta = 25.008$)	99.7% ($\theta = 25.242$)	99.8% ($\theta = 25.008$)
Data/restraints/parameters	14 818/0/1009	7999/0/493	8832/5/496	8002/6/487
GOF	0.963	1.049	1.043	1.030
Final R_1, wR_2 indices	0.0399, 0.1006	0.0363, 0.1003	0.0315, 0.0971	0.0377, 0.0974
R_1, wR_2 indices (all data)	0.0454, 0.1044	0.0448, 0.1059	0.0412, 0.1007	0.0465, 0.1020
Largest diff. peak and hole (e Å^{-3})	1.492 and −1.009	1.563 and −0.981	1.048 and −0.805	1.814 and −0.783

dehyde and 2-[*O*-(1-ethyloxyamide)]oxime-2-naphthol were prepared according to analogous methods reported earlier.[10]

An ethanol solution (10 mL) of 2,3-dihydroxybenzene-1,4-dicarbaldehyde (166.2 mg, 1.0 mmol) was added to an ethanol solution (20 mL) of 2-[*O*-(1-ethyloxyamide)]oxime-2-naphthol (492.6 mg, 2 mmol). The mixed solution was stirred at 55 °C for 8 h, cooling to room temperature, the precipitate was filtered and washed with *n*-hexane to obtain a yellow powder. Yield: 87%. mp.: 198–200 °C. Anal. calc. for $C_{34}H_{30}N_4O_8$: C, 65.59; H, 4.86; N, 9.00%. Found: C, 65.65; H, 4.94; N, 8.92%. ^{1}H NMR (400 MHz, $CDCl_3$) δ 10.82 (s, 2H), 9.70 (s, 2H), 9.17 (s, 2H), 8.25 (d, J = 2.5 Hz, 2H), 7.96 (d, J = 8.7 Hz, 2H), 7.80–7.72 (m, 4H), 7.50 (t, J = 7.7 Hz, 2H), 7.35 (t, J = 7.5 Hz, 2H), 7.20 (d, J = 9.0 Hz, 2H), 6.75 (s, 2H), 4.56 (s, 8H).

2.3. General procedure for the preparation of complexes 1–4

The synthesis methods of complexes **2–4** are similar to that of complex **1** (Scheme 2). An ethanol solution (3 mL) of $Zn(OAc)_2 \cdot 2H_2O$ (13.155 mg, 0.065 mmol) was added to a chloroform solution (5 mL) of H_4L (18.675 mg, 0.03 mmol) under constant magnetic stirring, and an ethanol solution (3 mL) of $La(NO_3)_3 \cdot 6H_2O$ (4.33 mg, 0.015 mmol) was then added. The mixed solution was stirred for 15 minutes at room temperature and then filtered off, and the filtrate was transferred to a cillin bottle. Sealed the opening of the bottle with tinfoil and let it stand for two weeks, some block-like crystals suitable for X-ray diffraction were formed.

Complex **1**, yellow block-like crystals. Yield: 52%. Elemental analysis: anal. calc. for $[Zn_4(L)_2La(NO_3)_2(OEt)(H_2O)]$ ($C_{70}H_{59}LaZn_4N_{10}O_{24}$) (%): C, 46.08; H, 3.26; N, 7.68; Zn, 14.33; La, 7.61. Found (%): C, 46.19; H, 3.38; N, 7.53; Zn, 14.41; La, 7.48.

Complex **2**, yellow block-like crystals. Yield: 62%. Elemental analysis: anal. calc. for $[Zn_4(L)_2Ce(NO_3)_2(OMe)(MeOH)]$ ($C_{70}H_{59}CeZn_4N_{10}O_{24}$) (%): C, 46.05; H, 3.26; N, 7.67; Zn, 14.32; Ce, 7.67. Found (%): C, 46.12; H, 3.37; N, 7.56; Zn, 14.39; Ce, 7.81.

Complex **3**, yellow block-like crystals. Yield: 69%. Elemental analysis: anal. calc. for $[Zn_4(L)_2Pr(NO_3)_2(OEt)(EtOH)]$ ($C_{72}H_{63}PrZn_4N_{10}O_{24}$) (%): C, 46.62; H, 3.42; N, 7.55; Zn, 14.10; Pr, 7.60. Found (%): C, 46.79; H, 3.48; N, 7.50; Zn, 14.15; Pr, 7.68.

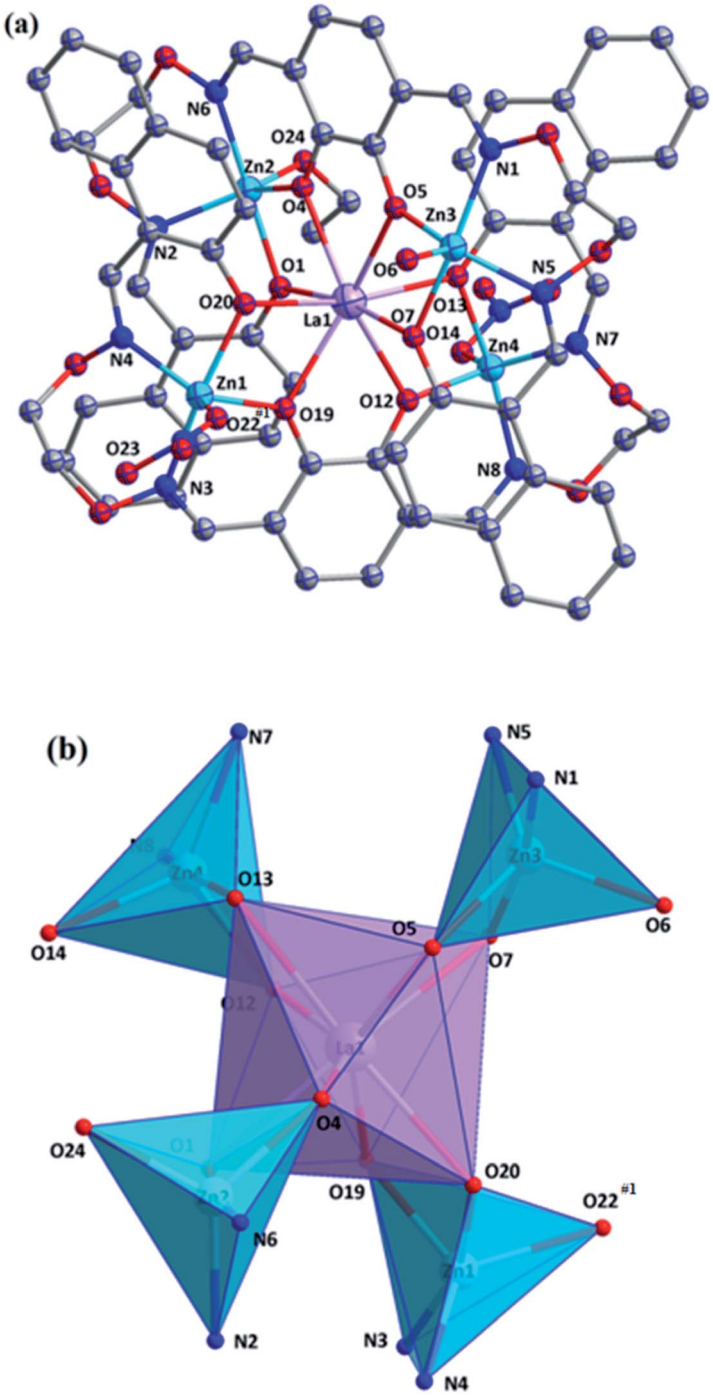

Fig. 3 (a) Molecule structure of complex **1** ($[Zn_4(L)_2La(NO_3)_2(OEt)(H_2O)]$) (hydrogen atoms and solvent molecules are omitted for clarity). (b) Coordination polyhedrons for Zn^{II} and La^{III} ions of complex **1**.

Complex **4**, yellow block-like crystals. Yield: 64%. Elemental analysis: anal. calc. for $[Zn_4(L)_2Nd(NO_3)_2(OMe)(MeOH)]$ ($C_{70}H_{59}NdZn_4N_{10}O_{24}$) (%): C, 45.94; H, 3.25; N, 7.65; Zn, 14.29; Nd, 7.88. Found (%): C, 46.09; H, 3.38; N, 7.53; Zn, 14.38; Nd, 7.96.

2.4. X-ray crystallographic analysis

Crystal data for complexes **1–4** were collected on a Bruker APEX-II CCD area detector with Mo Kα radiation (λ = 0.71073 Å) at 296(2), 173(2), 173(2) and 173(2) K. respectively. Reflection data were corrected for LP factors semi-empirical absorption were

Table 2 Selected bond lengths (Å) and angles (°) for complexes **1–4**[a]

Complex **1**

Bond	Lengths	Bond	Lengths	Bond	Lengths
Zn1–O19	2.001(3)	Zn1–O20	2.085(3)	Zn1–O22	2.054(6)
Zn2–O1	2.051(2)	Zn2–O4	1.957(2)	Zn1–O22$^{\#1}$	2.019(14)
Zn2–O24	2.014(3)	Zn3–O5	1.975(2)	Zn3–O6	1.983(3)
Zn3–O7	2.081(2)	Zn4–O12	1.999(3)	Zn4–O13	2.057(3)
Zn4–O14	2.059(3)	Zn1–N3	2.149(3)	Zn1–N4	2.048(3)
Zn2–N2	2.011(3)	Zn2–N6	2.108(3)	Zn3–N1	2.127(3)
Zn3–N5	2.019(3)	Zn4–N7	2.038(4)	Zn4–N8	2.120(3)
La1–O5	2.491(2)	La1–O12	2.497(2)	La1–O19	2.500(2)
La1–O20	2.496(3)	La1–O4	2.505(2)	La1–O7	2.514(2)
La1–O1	2.534(3)	La1–O13	2.537(3)		

Complex **1**

Bond	Angles	Bond	Angles	Bond	Angles
O19–Zn1–O22	109.0(2)	N4–Zn1–O22	123.2(2)	O19–Zn1–O20	81.62(10)
O19–Zn1–O22$^{\#1}$	134.0(5)	O19–Zn1–N4	124.08(12)	O22$^{\#1}$–Zn1–N4	101.9(4)
O22$^{\#1}$–Zn1–O20	105.3(4)	N4–Zn1–O20	83.62(11)	O22–Zn1–O20	85.79(17)
O19–Zn1–N3	86.56(12)	O22$^{\#1}$–Zn1–N3	89.3(4)	N4–Zn1–N3	95.80(14)
O22–Zn1–N3	106.58(18)	O20–Zn1–N3	165.20(13)	O4–Zn2–N2	129.50(12)
O4–Zn2–O24	109.62(13)	N2–Zn2–O24	120.27(14)	O4–Zn2–O1	83.74(10)
N2–Zn2–O1	85.55(11)	O24–Zn2–O1	93.95(12)	O4–Zn2–N6	89.59(11)
N2–Zn2–N6	95.24(12)	O24–Zn2–N6	92.61(13)	O1–Zn2–N6	171.90(12)
O5–Zn3–O6	113.02(12)	O5–Zn3–N5	128.10(12)	O6–Zn3–N5	117.44(14)
O5–Zn3–O7	83.24(10)	O6–Zn3–O7	90.74(12)	N5–Zn3–O7	84.77(11)
O5–Zn3–N1	87.25(11)	O6–Zn3–N1	97.52(14)	N5–Zn3–N1	97.33(13)
O7–Zn3–N1	169.29(12)	O12–Zn4–N7	124.57(13)	O12–Zn4–O13	82.80(10)
N7–Zn4–O13	84.94(12)	O12–Zn4–O14	103.94(11)	N7–Zn4–O14	130.82(13)
O13–Zn4–O14	94.37(12)	O12–Zn4–N8	87.66(12)	N7–Zn4–N8	96.06(14)
O13–Zn4–N8	169.00(13)	O14–Zn4–N8	93.24(14)		
O5–La1–O20	91.87(9)	O5–La1–O12	129.19(8)	O20–La1–O12	126.29(8)
O5–La1–O19	148.96(9)	O20–La1–O19	64.64(8)	O12–La1–O19	63.26(8)
O5–La1–O4	62.34(8)	O20–La1–O4	78.16(8)	O12–La1–O4	146.66(8)
O19–La1–O4	126.01(8)	O5–La1–O7	65.16(8)	O20–La1–O7	89.17(9)
O12–La1–O7	81.51(8)	O19–La1–O7	93.10(8)	O4–La1–O7	125.23(8)
O5–La1–O1	124.73(8)	O20–La1–O1	90.06(9)	O12–La1–O1	91.02(8)
O19–La1–O1	77.66(8)	O4–La1–O1	64.15(8)	O7–La1–O1	170.10(8)
O5–La1–O13	77.97(8)	O20–La1–O13	169.01(8)	O12–La1–O13	64.41(8)
O19–La1–O13	126.35(8)	O4–La1–O13	93.23(9)	O7–La1–O13	90.31(9)
O1–La1–O13	92.31(9)				

Complex **2**

Bond	Lengths	Bond	Lengths	Bond	Lengths
O12–Zn1	2.020(3)	O11–Zn1	2.043(2)	O10–Zn2	2.068(2)
O9–Zn2	2.026(3)	O4–Zn2	1.985(2)	O3–Zn1	1.972(2)
N4–Zn2	2.015(3)	N3–Zn2	2.137(3)	N2–Zn1	2.110(3)
N1–Zn1	2.019(3)				
Ce1–O3	2.475(2)	Ce1–O10$^{\#2}$	2.475(2)	Ce1–O11$^{\#2}$	2.511(2)
Ce1–O3$^{\#2}$	2.475(2)	Ce1–O4$^{\#2}$	2.479(2)	Ce1–O11	2.511(2)
Ce1–O10	2.475(2)	Ce1–O4	2.479(2)		

Complex **2**

Bond	Angles	Bond	Angles	Bond	Angles
O3–Zn1–O12	113.98(12)	O3–Zn1–N1	127.13(12)	O12–Zn1–N1	117.85(14)
O3–Zn1–O11	81.90(10)	O12–Zn1–O11	93.03(11)	N1–Zn1–O11	85.67(12)
O3–Zn1–N2	88.94(11)	O12–Zn1–N2	95.64(12)	N1–Zn1–N2	95.67(13)
O11–Zn1–N2	169.37(12)	O4–Zn2–N4	122.97(12)	O4–Zn2–O9	109.03(11)
N4–Zn2–O9	127.60(13)	O4–Zn2–O10	82.84(9)	N4–Zn2–O10	84.60(11)

Table 2 (*Contd.*)

Complex **2**

Bond	Angles	Bond	Angles	Bond	Angles
O9–Zn2–O10	96.52(12)	O4–Zn2–N3	87.24(11)	N4–Zn2–N3	95.14(13)
O9–Zn2–N3	93.18(14)	O10–Zn2–N3	167.93(12)		
O3–Ce1–O3$^{\#2}$	126.22(11)	O3$^{\#2}$–Ce1–O10	92.34(8)	O3$^{\#2}$–Ce1–O10$^{\#2}$	127.67(8)
O3–Ce1–O10	127.67(8)	O3–Ce1–O10$^{\#2}$	92.34(8)	O10–Ce1–O10$^{\#2}$	87.78(12)
O3–Ce1–O4$^{\#2}$	146.35(8)	O4$^{\#2}$–Ce1–O4	130.09(11)	O3–Ce1–O11	63.72(8)
O3$^{\#2}$–Ce1–O4$^{\#2}$	63.21(8)	O3–Ce1–O11$^{\#2}$	80.04(8)	O3$^{\#2}$–Ce1–O11	80.03(8)
O10–Ce1–O4$^{\#2}$	78.78(8)	O3$^{\#2}$–Ce1–O11$^{\#2}$	63.72(8)	O10–Ce1–O11	168.47(8)
O10$^{\#2}$–Ce1–O4$^{\#2}$	65.57(8)	O10–Ce1–O11$^{\#2}$	90.07(8)	O10$^{\#2}$–Ce1–O11	90.07(8)
O3–Ce1–O4	63.21(8)	O10$^{\#2}$–Ce1–O11$^{\#2}$	168.48(8)	O4$^{\#2}$–Ce1–O11	90.02(8)
O3$^{\#2}$–Ce1–O4	146.35(8)	O4$^{\#2}$–Ce1–O11$^{\#2}$	125.03(8)	O4–Ce1–O11	125.03(8)
O10–Ce1–O4	65.57(8)	O4–Ce1–O11$^{\#2}$	90.03(8)	O11$^{\#2}$–Ce1–O11	94.20(11)
O10$^{\#2}$–Ce1–O4	78.78(8)				

Complex **3**

Bond	Lengths	Bond	Lengths	Bond	Lengths
N1–Zn1	2.015(2)	N2–Zn1	2.143(3)	N3–Zn2	2.110(3)
N4–Zn2	2.018(3)	O1–Zn1	2.0699(19)	O5–Zn2	1.9785(19)
O8–Zn2	2.0372(19)	O12–Zn2	2.015(2)		
O1–Pr1	2.4646(19)	O8–Pr1	2.5097(19)	O5$^{\#3}$–Pr1	2.4471(19)
O4–Pr1	2.4605(19)	O1$^{\#3}$–Pr1	2.4646(19)	O8$^{\#3}$–Pr1	2.5097(19)
O5–Pr1	2.4471(19)	O4$^{\#3}$–Pr1	2.4605(19)		

Complex **3**

Bond	Angles	Bond	Angles	Bond	Angles
O4–Zn1–N1	122.13(9)	O4–Zn1–O9	110.45(9)	N1–Zn1–O9	127.21(10)
O4–Zn1–O1	82.56(8)	N1–Zn1–O1	85.70(9)	O9–Zn1–O1	97.27(9)
O4–Zn1–N2	86.69(9)	N1–Zn1–N2	94.43(10)	O9–Zn1–N2	92.74(10)
O1–Zn1–N2	167.33(9)	O5–Zn2–O12	113.73(10)	O5–Zn2–N4	126.50(9)
O12–Zn2–N4	118.79(11)	O5–Zn2–O8	81.60(8)	O12–Zn2–O8	93.65(9)
N4–Zn2–O8	85.60(9)	O5–Zn2–N3	89.31(9)	O12–Zn2–N3	94.94(10)
N4–Zn2–N3	95.59(10)	O8–Zn2–N3	169.44(9)		
O5$^{\#3}$–Pr1–O5	125.71(9)	O5$^{\#3}$–Pr1–O1$^{\#3}$	128.04(6)	O1–Pr1–O8$^{\#3}$	88.83(7)
O5$^{\#3}$–Pr1–O4	146.19(6)	O5–Pr1–O1$^{\#3}$	91.97(6)	O1$^{\#3}$–Pr1–O8$^{\#3}$	167.92(6)
O5–Pr1–O4	63.29(6)	O4–Pr1–O1$^{\#3}$	79.09(6)	O5$^{\#3}$–Pr1–O8	80.03(6)
O5$^{\#3}$–Pr1–O4$^{\#3}$	63.29(6)	O4$^{\#3}$–Pr1–O1$^{\#3}$	65.99(6)	O5–Pr1–O8	63.92(6)
O5–Pr1–O4$^{\#3}$	146.19(6)	O1–Pr1–O1$^{\#3}$	89.04(9)	O4–Pr1–O8	125.13(6)
O4–Pr1–O4$^{\#3}$	130.59(9)	O5$^{\#3}$–Pr1–O8$^{\#3}$	63.92(6)	O4$^{\#3}$–Pr1–O8	89.19(6)
O5$^{\#3}$–Pr1–O1	91.97(6)	O5–Pr1–O8$^{\#3}$	80.03(6)	O1–Pr1–O8	167.93(6)
O5–Pr1–O1	128.04(6)	O4–Pr1–O8$^{\#3}$	89.19(6)	O1$^{\#3}$–Pr1–O8	88.83(7)
O4–Pr1–O1	65.99(6)	O4$^{\#3}$–Pr1–O8$^{\#3}$	125.13(6)	O8$^{\#3}$–Pr1–O8	95.65(9)
O4$^{\#3}$–Pr1–O1	79.10(6)				

Complex **4**

Bond	Lengths	Bond	Lengths	Bond	Lengths
N1–Zn1	2.020(3)	N2–Zn1	2.110(3)	N3–Zn2	2.133(3)
N4–Zn2	2.017(3)	O3–Zn1	1.968(3)	O4–Zn2	1.985(2)
O9–Zn2	2.023(3)	O10–Zn2	2.061(3)	O11–Zn1	2.046(3)
O12–Zn1	2.017(3)				
Nd1–O4	2.444(2)	Nd1–O3	2.450(2)	Nd1–O11$^{\#4}$	2.481(3)
Nd1–O4$^{\#4}$	2.444(2)	Nd1–O10	2.452(2)	Nd1–O11	2.481(3)
Nd1–O3$^{\#4}$	2.450(2)	Nd1–O10$^{\#4}$	2.452(2)		

Table 2 (*Contd.*)

Complex **4**

Bond	Angles	Bond	Angles	Bond	Angles
O3–Zn1–O12	113.61(13)	O3–Zn1–N1	127.19(13)	O12–Zn1–N1	118.26(15)
O3–Zn1–O11	81.28(10)	O12–Zn1–O11	93.77(12)	N1–Zn1–O11	86.07(12)
O3–Zn1–N2	89.29(12)	O12–Zn1–N2	95.15(13)	N1–Zn1–N2	95.29(14)
O11–Zn1–N2	169.03(13)	O4–Zn2–N4	122.85(13)	O4–Zn2–O9	109.21(11)
N4–Zn2–O9	127.58(13)	O4–Zn2–O10	82.07(10)	N4–Zn2–O10	85.26(12)
O9–Zn2–O10	96.81(13)	O4–Zn2–N3	87.26(12)	N4–Zn2–N3	94.59(14)
O9–Zn2–N3	93.47(14)	O10–Zn2–N3	167.13(12)		
O4–Nd1–$O4^{\#4}$	129.52(12)	O4–Nd1–$O10^{\#4}$	78.43(9)	O10–Nd1–$O11^{\#4}$	90.19(9)
O4–Nd1–$O3^{\#4}$	145.82(8)	$O4^{\#4}$–Nd1–$O10^{\#4}$	65.72(8)	$O10^{\#4}$–Nd1–$O11^{\#4}$	167.33(8)
$O4^{\#4}$–Nd1–$O3^{\#4}$	63.98(8)	$O3^{\#4}$–Nd1–$O10^{\#4}$	128.56(8)	O4–Nd1–O11	126.22(8)
O4–Nd1–O3	63.98(8)	O3–Nd1–$O10^{\#4}$	91.74(8)	$O4^{\#4}$–Nd1–O11	89.50(8)
$O4^{\#4}$–Nd1–O3	145.82(8)	O10–Nd1–$O10^{\#4}$	88.34(12)	$O3^{\#4}$–Nd1–O11	79.37(8)
$O3^{\#4}$–Nd1–O3	125.79(12)	O4–Nd1–$O11^{\#4}$	89.50(8)	O3–Nd1–O11	64.06(9)
O4–Nd1–O10	65.72(8)	$O4^{\#4}$–Nd1–$O11^{\#4}$	126.21(8)	O10–Nd1–O11	167.33(8)
$O4^{\#4}$–Nd1–O10	78.43(9)	$O3^{\#4}$–Nd1–$O11^{\#4}$	64.06(8)	$O10^{\#4}$–Nd1–O11	90.20(9)
$O3^{\#4}$–Nd1–O10	91.73(8)	O3–Nd1–$O11^{\#4}$	79.37(8)	$O11^{\#4}$–Nd1–O11	93.93(12)
O3–Nd1–O10	128.56(8)				

[a] Symmetry transformations used to generate equivalent atoms: $^{\#1}3/2 - x, -1/2 + y, 3/2 - z$; $^{\#2} - x + 1, y, -z + 1/2$; $^{\#3} - x, y, -z + 1/2$; $^{\#4} - x + 1, y, -z + 1/2$.

using SADABS. The single crystal structures were solved by the direct methods (SHELXS-2016).[11a] All hydrogen atoms were included at the calculated positions, and their positions were refined by a riding model. All non-hydrogen atoms were refined anisotropically using a full-matrix least-squares procedure on F^2 with SHELXL-2016.[11b] Crystallographic data and the structure refinements for complexes **1–4** are presented in Table 3.

3 Results and discussion

3.1. IR spectra

IR spectra of H_4L and its corresponding complexes **1–4** displayed various bands in the 4000–400 cm^{-1} region (Fig. 1).

In the infrared spectrum of H_4L, a typical C=N stretching band appeared at *ca.* 1603 cm^{-1}, and C=N stretching bands of complexes **1–4** were observed at 1609–1614 cm^{-1}, indicating that H_4L has coordinated with Zn^{II} ions.[12] In addition, the free ligand H_4L exhibited a typical Ar–O stretching frequency at *ca.* 1239 cm^{-1}, while the Ar–O stretching frequencies in complexes **1–4** were observed at *ca.* 1232, 1235, 1231 and 1232 cm^{-1}, which are shifted to lower frequencies, indicating that the Zn–O or Ln–O bond is formed between the oxygen atoms of phenolic group and the metal ions.[13] Meanwhile, the hydroxyl stretching band of H_4L was observed at *ca.* 3435 cm^{-1} that belongs to the phenolic O–H groups. These absorption bands in complexes **1–4** were observed at *ca.* 3441–3443 cm^{-1}, indicating the existence of coordinated water, methanol or ethanol molecules.[14]

3.2. UV-Vis spectra

The UV-Vis absorption spectra of H_4L and its complexes **1–4** in $CHCl_3/CH_3CH_2OH$ solution (v/v = 1 : 1) are shown in Fig. 2. The absorption spectrum of H_4L (1.0×10^{-5} M) showed four relatively strong absorption peaks at *ca.* 302, 313, 341 and 355 nm, the former two peaks can be assigned to the π–π* transitions of the naphthalene rings. The later two absorption peaks can be assigned to the intra-ligand π–π* transition of the oxime group.[15] Compared with the absorption peaks of the free ligand H_4L, the first absorption peaks were observed at 326, 325, 321 and 325 nm in complexes **1–4**, respectively. These peaks are bathochromically shifted, indicating coordination of the $(L)^{4-}$ moieties with metal(II/III) ions. Meanwhile, the new peaks emerged at *ca.* 382 nm in complexes **1–4**, respectively, which belong to the n–π* charge transfer transitions from the lone-pair electrons of the N atoms of C=N groups to benzene rings.[16]

3.3. Crystal structure descriptions

X-ray crystallographic analysis revealed the crystal structures of complexes **1–4**. Selected bond lengths and angles are given in Table 1

3.3.1. Crystal structure of complex 1. The crystallographic data revealed that complex **1** ($[Zn_4(L)_2La(NO_3)_2(OEt)(H_2O)]$) was a hetero-pentanuclear complex, crystallizes in the monoclinic system, space group *C*2/*c*, and consists of four Zn^{II} ions, one La^{III} ion, two $(L)^{4-}$ units, one coordinated ethoxy group, one coordinated water molecule and two nitrate groups (Fig. 3). N_2O_2 sites of the salamo moieties were occupied by four Zn^{II} ions (Zn1, Zn2, Zn3 and Zn4), the Zn^{II} ions were located in N_2O_3 coordination spheres, and assumed trigonal bipyramid coordination environment ($\tau_1 = 0.68$, $\tau_2 = 0.71$, $\tau_3 = 0.69$ and $\tau_4 = 0.64$).[17] Meanwhile, the eight phenoxo donors (O1, O4, O5, O7, O12, O13, O19 and O20) from two completely deprotonated $(L)^{4-}$ units as a central O_8 site coordinated to La^{III} ion, the La^{III}

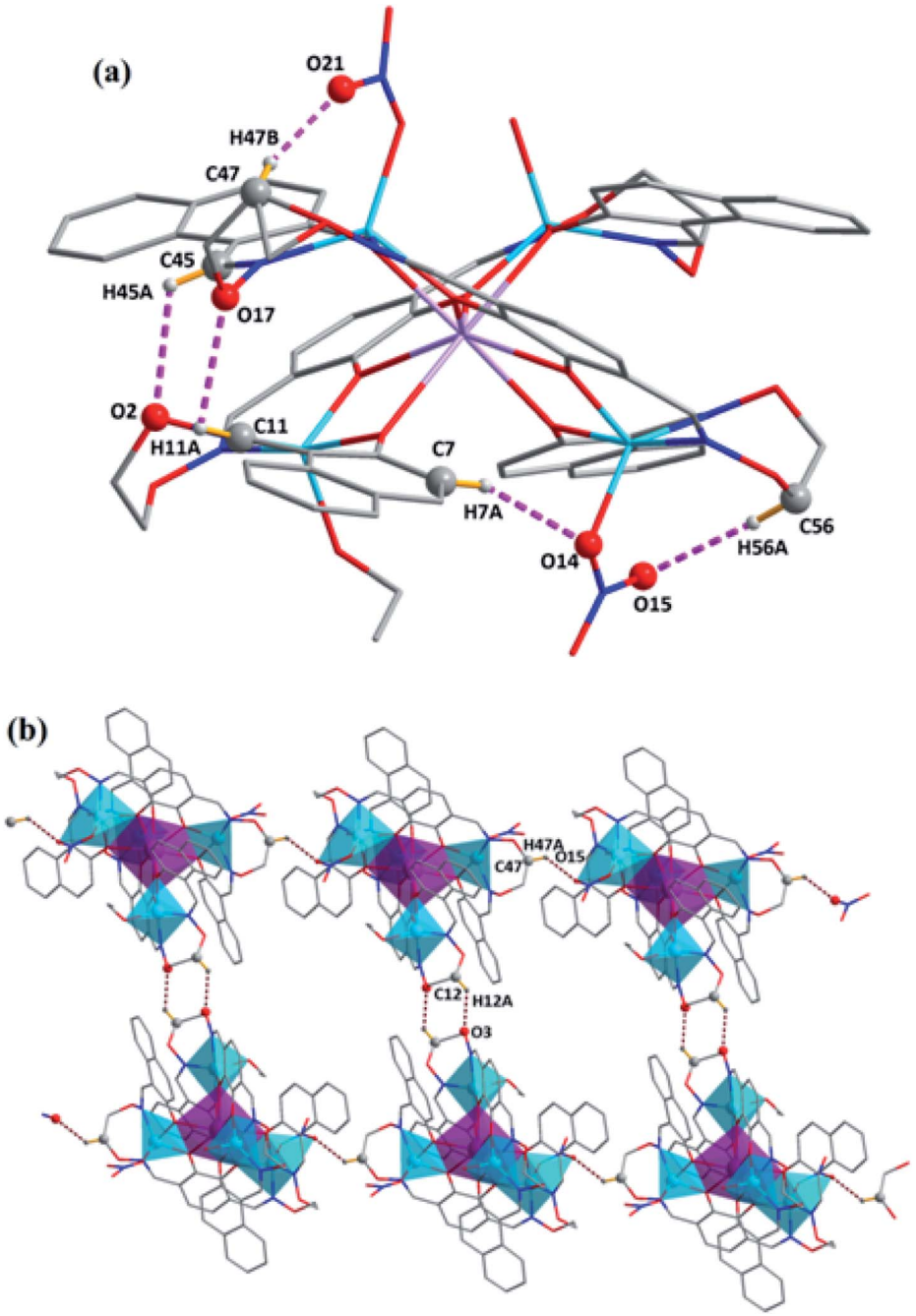

Fig. 4 (a) View of the intramolecular hydrogen bonding interactions of complex **1**. (b) View of an infinite 2D supramolecular structure of complex **1**.

ion lay in an O_8 coordination sphere, and adopted a distorted square antiprismatic coordination environment. Finally, complex **1** formed a rare heteropentanuclear 3d–4f complex.[18] The distances of Zn···La1, Zn–N, Zn–O and La1–O bonds are in the ranges of 3.6130(5)–3.6513(5), 2.011(3)–2.149(3), 1.957(2)–2.085(3) and 2.491(2)–2.537(3) Å, respectively.

The intramolecular and intermolecular hydrogen bonds for complex **3** are presented in Table 2. Each molecule formed five intramolecular hydrogen bonds (C23–H23A···O12 and C8–H8A···O10) as shown in Fig. 4.[19] Meanwhile, a self-assembled infinite 2D supramolecular structure was formed by C12–H12A···O3 and C47–H47A···O15 hydrogen bond interactions[20] (Fig. 4).

3.3.2. Crystal structure of complex 2. The crystallographic data revealed that complex **2** ($[Zn_4(L)_2Ce(NO_3)_2(OMe)(MeOH)]$) crystallizes in the monoclinic system, space group *C*2/*c*. Unlike complex **1**, it consists of four Zn^{II} ions, one Ce^{III} ion, two ligand $(L)^{4-}$ units, one coordinated methoxo group, one coordinated

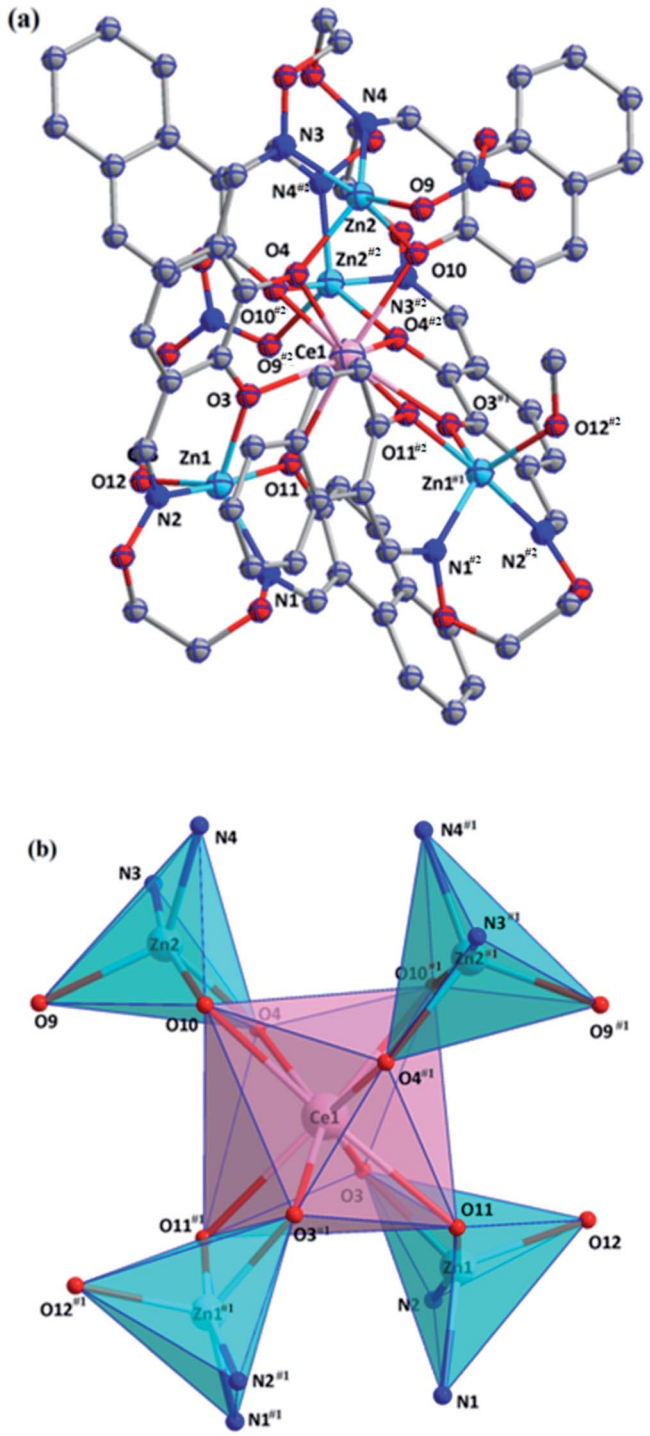

Fig. 5 (a) Molecule structure of complex **2** ($[Zn_4(L)_2Ce(NO_3)_2(OMe)(MeOH)]$) (hydrogen atoms and solvent molecules are omitted for clarity). (b) Coordination polyhedrons for Zn^{II} and Ce^{III} ions of complex **2**.

methanol molecule and two monodentate nitrate groups (Fig. 5).

Zn1 and Zn2 ions were located in penta-coordinated spheres and adopted trigonal bipyramid coordination environments ($\tau_1 = 0.704$ and $\tau_2 = 0.67$).[17] The coordination number of Ce^{III} ion is 8, consisting of eight phenolic oxygen atoms from two full deprotonated $(L)^{4-}$ units and adopted a distorted square antiprismatic coordination environment (Fig. 5).[18]

In the crystal structure of complex **2**, there were many intramolecular hydrogen bonds (C2–H2···O9, C11–H11···O1 and C22–H22A···O7).[19] As shown in Fig. 6. Moreover, the 2D supramolecular structure was formed by C12–H12A···O7 hydrogen bonding interactions in complex **2** (ref. 21) (Fig. 6).

3.3.3. Crystal structure of complex 3. Complex **3** ($[Zn_4(L)_2Pr(NO_3)_2(OEt)(EtOH)]$) crystallizes in the monoclinic crystal system, space group *C*2/*c*. X-ray crystallography clearly showed the formation of complex **3**. Different from complexes **1** and **2**, it consists of four Zn^{II} ions, one Pr^{III} ion, two ligand $(L)^{4-}$ units, one coordinated ethoxy group, one coordinated ethanol molecule and two monodentate nitrate groups (Fig. S2†).

The Zn^{II} ions also were located in the N_2O_2 sites, and four Zn^{II} ions are also penta-coordinated. The Zn^{II} ions (Zn1 and Zn2) adopted trigonal bipyramid coordination environment ($\tau_1 = 0.67$ and $\tau_2 = 0.72$).[17] The Pr^{III} ion was also located in the O_8 site that consists of eight phenoxo oxygen atoms, forming a distorted square antiprismatic coordination environment.[18]

The main interactions in complex **3** are listed in Table 3, four pairs of intramolecular hydrogen bonds (C13–H13B···O10, C24–H24···O7, C27–H27···O9 and C35–H35B···O11) were formed.[19] Besides, The O10 atom of nitrate group as acceptor formed a hydrogen bond with the donor (C23H23B–) in complex **3**, which adopted a 2D supramolecular structure[22] (Fig. S3†).

3.3.4. Crystal structure of complex 4. As shown in Fig. S4,† X-ray crystallographic analysis of complex **4** ($[Zn_4(L)_2Nd(NO_3)_2(OMe)(MeOH)]$) revealed that crystallizes in the monoclinic system, space group *C*2/*c*. Similar to the structure of complex **2**, it consists of four Zn^{II} ions, one Nd^{III} ion, two ligand $(L)^{4-}$ units, one coordinated methoxo group, one coordinated methanol molecule and two monodentate nitrate groups.

All Zn^{II} ions lay in N_2O_3 coordination spheres. The Zn1 and Zn2 ($Zn1^{\#4}$ and $Zn2^{\#4}$) ions were all made of the N_2O_2 cavities and one coordinated nitrate group, which assumed trigonal bipyramid coordination environments ($\tau_1 = 0.69$ and $\tau_2 = 0.66$).[17] The Nd^{III} ion exhibited an O_8 coordination sphere, which is made of eight phenoxo donors (O3, O4, O10, O11, $O3^{\#4}$, $O4^{\#4}$, $O10^{\#4}$ and $O11^{\#4}$) from two completely deprotonated $(L)^{4-}$ units, while the central Nd^{III} ion is octa-coordinated with a distorted square antiprismatic coordination environment.[18]

In complex **4**, three pairs of significant intramolecular hydrogen bonds (C2–H2A···O9, C11–H11···O1 and C22–H22A···O7) were formed[19] (Fig. S5(a)†). Meanwhile, complex **4** molecules formed a 2D supramolecular structure by intermolecular hydrogen bonds (C6–H6···O8 and C12–H12A···O7)[23] (Fig. S5(b)†).

3.4. Spectroscopic properties

The free ligand H_4L and its corresponding complexes **1–4** were excited at 385 nm (λ_{ex}) respectively (Fig. 7). The emission

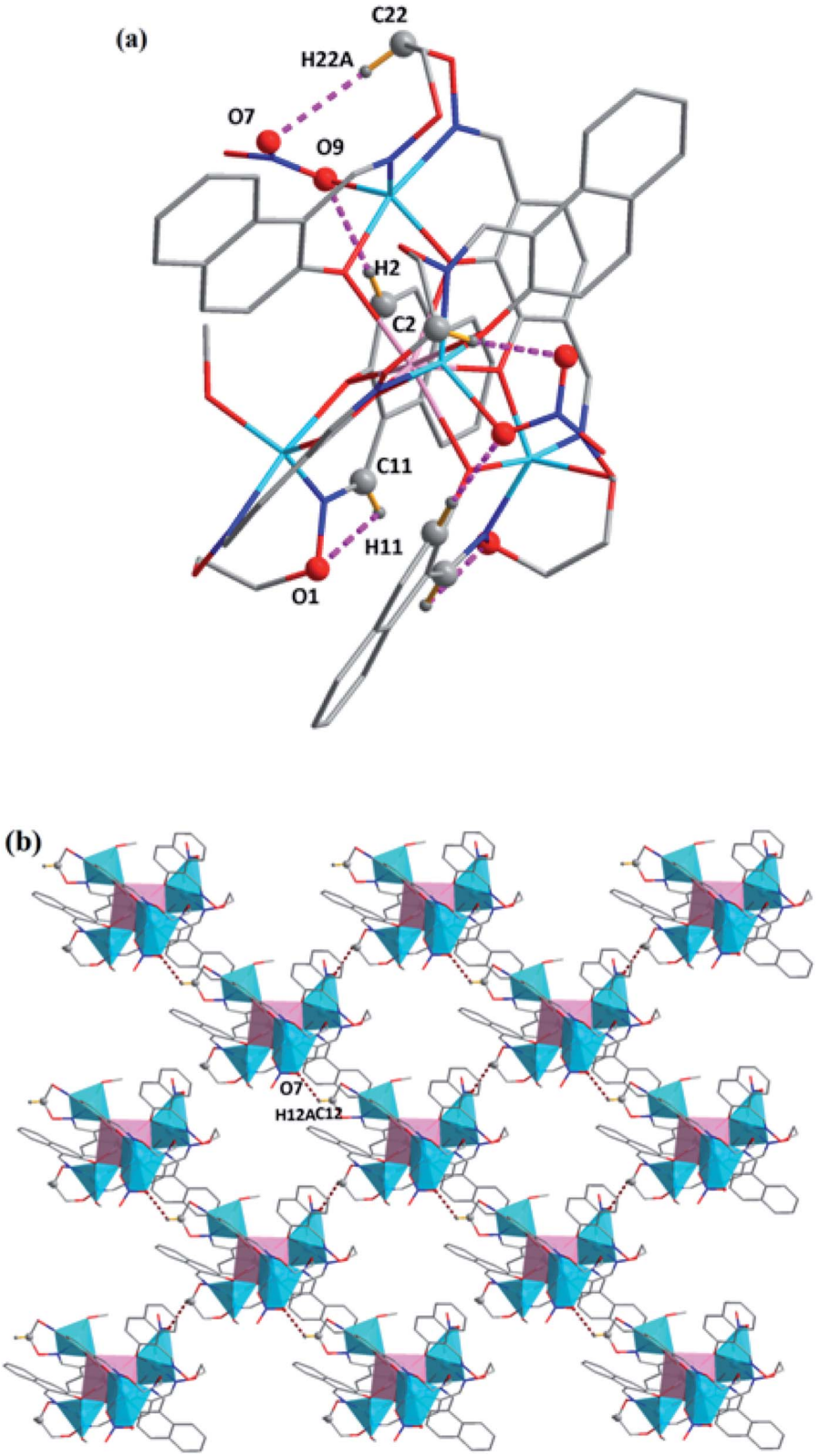

Fig. 6 (a) View of the intramolecular hydrogen bonding interactions of complex **2**. (b) View of an infinite 2D supramolecular structure of complex **2**.

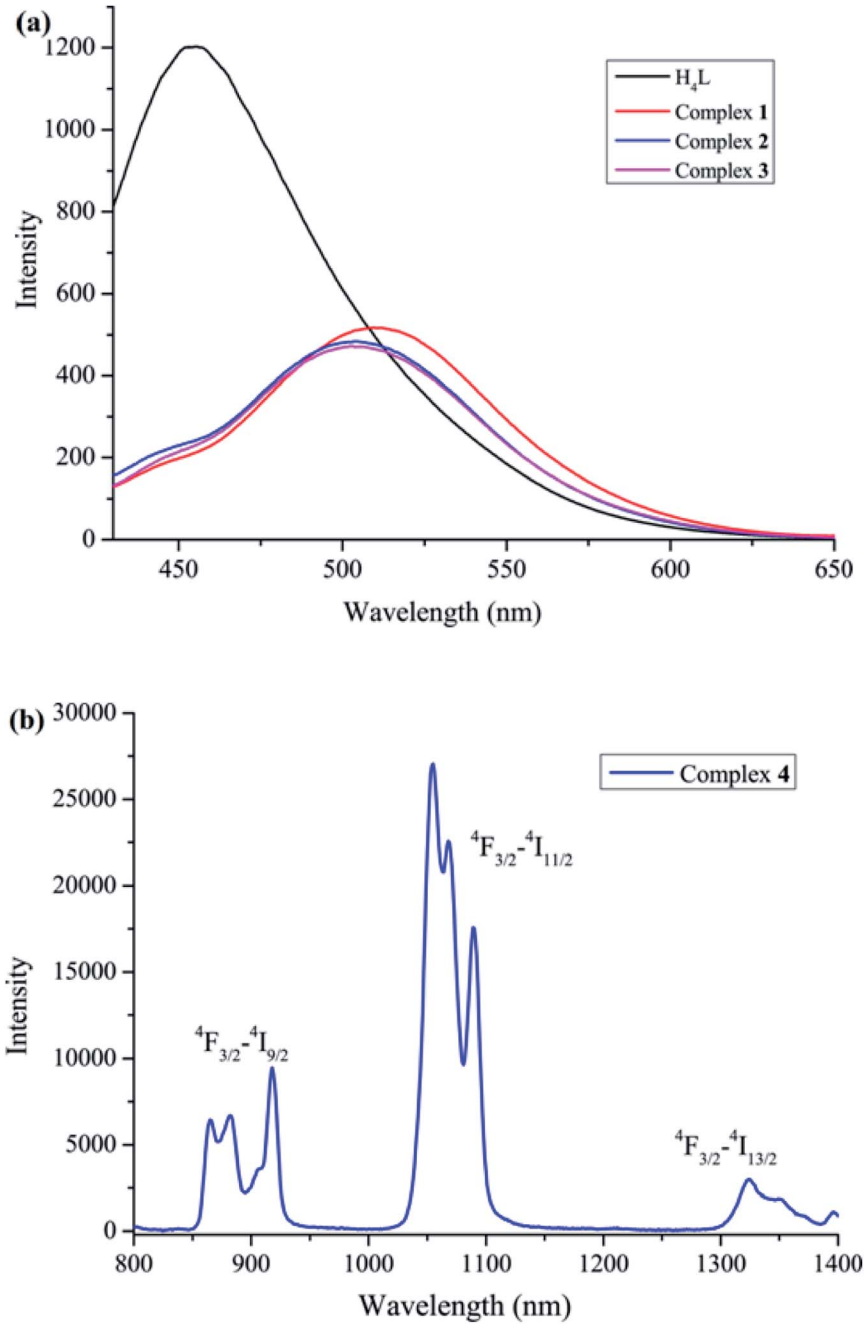

Fig. 7 (a) Visible luminescence spectra of complexes **1–3**. (b) NIR luminescence spectrum of complex **4**.

spectrum of H_4L exhibited a broad emission band, and the emission maximum at 454 nm, which can be assigned to the π–π* electronic transitions in the ligand.[24] Compared to H_4L, the absorption peaks of complexes **1–3** are bathochromically-shifted, which is may originated from the LMCT emission.

Due to energy mismatch, complexes **1–3** have no NIR luminescence. The NIR luminescence spectrum of complex **4** excited at 385 nm showed the characteristic emitting peaks at *ca.* 871, 917, 1055 and 1324 nm (Fig. 7(b)). These emission peaks are typical peaks of Nd^{III} ions, and correspond to $^4F_{3/2} \rightarrow {}^4I_{9/2}$, $^4F_{3/2} \rightarrow {}^4I_{11/2}$ and $^4F_{3/2} \rightarrow {}^4I_{13/2}$ transitions.[25] The ligand $(L)^{4-}$ units could serve as sensitizing agent for Nd^{III} luminescence in the NIR region.

4 Conclusions

In this work, four rare hetero-pentanuclear 3d–4f complexes of a bis(salamo)-type ligand (H_4L) have been synthesized and structurally characterized. In complexes **1–4**, all four Zn^{II} ions presented N_2O_3 coordination spheres. The Ln^{III} ion exhibited an O_8 coordination sphere, and assumed a distorted square

Table 3 Hydrogen bonding distances (Å) and bond angles (°) for complexes **1–4**

D–H···A	*d*(D–H)	*d*(H–A)	*d*(D–A)	∠D–X–A	Sum
Complex 1					
C7–H7A···O14	0.93	2.55	3.436(5)	159	
C47–H47B···O21	0.97	1.89	2.653(12)	134	
C56–H56A···O15	0.97	2.54	3.507(8)	174	
C12–H12A···O3	0.97	2.44	3.214(5)	137	$1 - x, 1 - y, 1 - z$
C47–H47A···O15	0.97	2.56	3.244(8)	128	$-1/2 + x, 1/2 + y, z$
Complex 2					
C2–H2···O9	0.95	2.51	3.451(5)	173	$1 - x, y, 1/2 - z$
C22–H22A···O7	0.99	2.51	3.490(6)	172	
Complex 3					
C13–H13B···O10	0.99	2.53	3.516(4)	173	
C23–H23B···O10	0.99	2.54	3.148(4)	120	$1/2 + x, 1/2 + y, z$
C27–H27···O9	0.95	2.50	3.448(4)	175	$-x, y, 1/2 - z$
C35–H35B···O11	0.98	2.58	3.438(8)	146	$-x, y, 1/2 - z$
Complex 4					
C2–H2A···O9	0.95	2.51	3.456(6)	172	$1 - x, y, 1/2 - z$
C6–H6···O8	0.95	2.56	3.361(11)	142	$-1/2 + x, 1/2 - y, -1/2 + z$
C22–H22A···O7	0.99	2.52	3.499(6)	172	

antiprismatic coordination environment. In a conclusion, the studies demonstrated that incorporation of salamo-like ligand was an optimistic approach to build Zn^{II}–Ln^{III} complexes which can display excellent spectroscopic resting with the lanthanide ions used.

Conflicts of interest

There are no conflicts to declare.

Acknowledgements

This work was supported by the National Natural Science Foundation of China (21761018), Science and Technology Program of Gansu Province (18YF1GA054) and the Program for Excellent Team of Scientific Research in Lanzhou Jiaotong University (201706), three of which are gratefully acknowledged.

References

1 (*a*) Y. X. Sun, L. Xu, T. H. Zhao, S. H. Liu, G. H. Liu and X. T. Dong, *Synth. React. Inorg., Met.-Org., Nano-Met. Chem.*, 2013, **43**, 509–513; (*b*) Y. X. Sun, S. T. Zhang, Z. L. Ren, X. Y. Dong and L. Wang, *Synth. React. Inorg., Met.-Org., Nano-Met. Chem.*, 2013, **43**, 995–1000; (*c*) Y. X. Sun and X. H. Gao, *Synth. React. Inorg., Met.-Org., Nano-Met. Chem.*, 2011, **41**, 973–978; (*d*) Y. X. Sun, L. Wang, X. Y. Dong, Z. L. Ren and W. S. Meng, *Synth. React. Inorg., Met.-Org., Nano-Met. Chem.*, 2013, **43**, 599–603; (*e*) Y. X. Sun, R. E. Lu, X. R. Li, Y. Y. Zhao and C. Y. Li, *Chin. J. Inorg. Chem.*, 2015, **31**, 1055–1062; (*f*) G. Murugavel, P. Sadhu and T. Punniyamurthy, *Chem. Rec.*, 2016, **16**, 1906–1917; (*g*) A. B. Canaj, M. Siczek, M. Otręba, T. Lis, G. Lorusso, M. Evangelisti and C. J. Milioset, *Dalton Trans.*, 2016, **45**, 18591–18602.

2 (*a*) L. Q. Chai, J. J. Huang, J. Y. Zhang and Y. X. Li, *J. Coord. Chem.*, 2015, **68**, 1224–1237; (*b*) L. Q. Chai, K. Y. Zhang, L. J. Tang, J. Y. Zhang and H. S. Zhang, *Polyhedron*, 2017, **130**, 100–107; (*c*) L. Q. Chai, L. J. Tang, L. C. Chen and J. J. Huang, *Polyhedron*, 2017, **122**, 228–240; (*d*) L. Q. Chai, G. Liu, J. Y. Zhang, J. J. Huang and J. F. Tong, *J. Coord. Chem.*, 2013, **66**, 3926–3938; (*e*) L. Q. Chai, J. J. Huang and H. S. Zhang, *Spectrochim. Acta, Part A*, 2014, **131**, 526–533.

3 (*a*) Q. Zhao, Z. L. Wei, Q. P. Kang, H. Zhang and W. K. Dong, *Spectrochim. Acta, Part A*, 2018, **203**, 472–480; (*b*) L. Chen, W. K. Dong, H. Zhang, Y. Zhang and Y. X. Sun, *Cryst. Growth Des.*, 2017, **17**, 3636–3648; (*c*) Y. D. Peng, F. Wang, L. Gao and W. K. Dong, *J. Chin. Chem. Soc.*, 2018, **65**, 893–899; (*d*) X. Y. Dong, Q. P. Kang, X. Y. Li, J. C. Ma and W. K. Dong, *Crystals*, 2018, **8**, 139; (*e*) L. Z. Liu, M. Yu, X. Y. Li, Q. P. Kang and W. K. Dong, *Chin. J. Inorg. Chem.*, 2019, **35**, 1283–1294.

4 (*a*) X. Y. Li, L. Chen, L. Gao, Y. Zhang, S. F. Akogun and W. K. Dong, *RSC Adv.*, 2017, **7**, 35905–35916; (*b*) L. H. Li, W. K. Dong, Y. Zhang, S. F. Akogun and L. Xu, *Appl. Organomet. Chem.*, 2017, e3818.

5 (*a*) X. Q. Song, P. P. Liu, Z. R. Xiao, X. Li and Y. A. Liu, *Inorg. Chim. Acta*, 2015, **438**, 232–244; (*b*) Y. A. Liu, C. Y. Wang, M. Zhang and X. Q. Song, *Polyhedron*, 2017, **127**, 278–286; (*c*) P. P. Liu, L. Sheng, X. Q. Song, W. Y. Xu and Y. A. Liu, *Inorg. Chim. Acta*, 2015, **434**, 252–257.

6 (*a*) H. L. Wu, G. L. Pan, Y. C. Bai, H. Wang, J. Kong, F. R. Shi, Y. H. Zhang and X. L. Wang, *J. Chem. Res.*, 2014, **38**, 211–217; (*b*) H. L. Wu, Y. C. Bai, Y. H. Zhang, G. L. Pan, J. Kong, F. R. Shi and X. L. Wang, *Z. Anorg. Allg. Chem.*, 2014, **640**, 2062–2071; (*c*) H. L. Wu, G. L. Pan, Y. C. Bai, Y. H. Zhang, H. Wang, F. R. Shi, X. L. Wang and J. Kong, *J. Photochem.*

Photobiol., B, 2014, **135**, 33–43; (*d*) H. L. Wu, C. P. Wang, F. Wang, H. P. Peng, H. Zhang and Y. C. Bai, *J. Chin. Chem. Soc.*, 2015, **62**, 1028–1034; (*e*) H. L. Wu, Y. C. Bai, Y. H. Zhang, Z. Li, M. C. Wu, C. Y. Chen and J. W. Zhang, *J. Coord. Chem.*, 2014, **67**, 3054–3066; (*f*) H. L. Wu, G. L. Pan, Y. C. Bai, H. Wang, J. Kong, F. R. Shi, Y. H. Zhang and X. L. Wang, *Res. Chem. Intermed.*, 2015, **41**, 3375–3383; (*g*) C. Y. Chen, J. W. Zhang, Y. H. Zhang, Z. H. Yang, H. L. Wu, G. L. Pana and Y. C. Bai, *J. Coord. Chem.*, 2015, **68**, 1054–1071; (*h*) H. L. Wu, Y. Bai, J. K. Yuan, H. Wang, G. L. Pan, X. Y. Fan and J. Kong, *J. Coord. Chem.*, 2012, **65**, 2839–2851.

7 (*a*) L. W. Zhang, L. Z. Liu, F. Wang and W. K. Dong, *Molecules*, 2018, **23**, 1141; (*b*) F. Wang, L. Gao, Q. Zhao, Y. Zhang, W. K. Dong and Y. J. Ding, *Spectrochim. Acta, Part A*, 2018, **190**, 111–115; (*c*) J. Hao, X. Y. Li, Y. Zhang and W. K. Dong, *Materials*, 2018, **11**, 523; (*d*) F. Wang, L. Z. Liu, L. Gao and W. K. Dong, *Spectrochim. Acta, Part A*, 2018, **203**, 56–64; (*e*) L. Z. Liu, L. Wang, M. Yu, Q. Zhao, Y. Zhang, Y. X. Sun and W. K. Dong, *Spectrochim. Acta, Part A*, 2019, **222**, 117209.

8 (*a*) S. S. Zheng, W. K. Dong, Y. Zhang, L. Chen and Y. J. Ding, *New J. Chem.*, 2017, **41**, 4966–4973; (*b*) Q. P. Li, Y. Peng, J. J. Qian, T. Yan, L. Du and Q. H. Zhao, *Dalton Trans.*, 2019, **48**, 12880–12887; (*c*) J. J. Qian, T. T. Li, Y. Hua and S. M. Huang, *Chem. Commun.*, 2017, **53**, 13027–13030; (*d*) J. J. Qian, Q. P. Li, L. F. Liang, Y. Yang, Z. Cao, P. P. Yu, S. M. Huang and M. C. Hong, *Chem. Commun.*, 2016, **52**, 9032–9035.

9 X. Y. Dong, Q. Zhao, Q. P. Kang, X. Y. Li and W. K. Dong, *Crystals*, 2018, **8**, 230.

10 (*a*) S. Akine, T. Taniguchi, W. K. Dong, S. Masubuchi and T. Nabeshima, *J. Org. Chem.*, 2005, **70**, 1704–1711; (*b*) J. Hao, X. Y. Li, L. Wang, Y. Zhang and W. K. Dong, *Spectrochim. Acta, Part A*, 2018, **204**, 388–402.

11 (*a*) G. M. Sheldrick, *SHELXS-2016, Program for crystal structure solution*, University of Göttingen, Göttingen Germany, 2016; (*b*) G. M. Sheldrick, *SHELXL-2016, Program for crystal structure refinement*, University of Göttingen, Göttingen Germany, 2016.

12 (*a*) X. Y. Dong, Y. X. Sun, L. Wang and L. Li, *J. Chem. Res.*, 2012, **36**, 387–390; (*b*) Z. L. Ren, J. Hao, P. Hao, X. Y. Dong, Y. Bai and W. K. Dong, *Z. Naturforsch.*, 2018, **73b**, 203–210; (*c*) L. Xu, L. C. Zhu, J. C. Ma, Y. Zhang, J. Zhang and W. K. Dong, *Z. Anorg. Allg. Chem.*, 2015, **641**, 2520–2524.

13 (*a*) L. Wang, J. Hao, L. X. Zhai, Y. Zhang and W. K. Dong, *Crystals*, 2017, **7**, 277; (*b*) J. Chang, H. J. Zhang, H. R. Jia and Y. X. Sun, *Chin. J. Inorg. Chem.*, 2018, **34**, 2097–2107.

14 (*a*) L. Gao, F. Wang, Q. Zhao, Y. Zhang and W. K. Dong, *Polyhedron*, 2018, **139**, 7–16; (*b*) L. W. Zhang, X. Y. Li, Q. P. Kang, L. Z. Liu, J. C. Ma and W. K. Dong, *Crystals*, 2018, **8**, 173.

15 (*a*) Q. P. Kang, X. Y. Li, Q. Zhao, J. C. Ma and W. K. Dong, *Appl. Organomet. Chem.*, 2018, **32**, e4379; (*b*) X. Y. Li, Q. P. Kang, L. Z. Liu, J. C. Ma and W. K. Dong, *Crystals*, 2018, **8**, 43; (*c*) Y. D. Peng, X. Y. Li, Q. P. Kang, G. X. An, Y. Zhang and W. K. Dong, *Crystals*, 2018, **8**, 107.

16 (*a*) L. Gao, C. Liu, F. Wang and W. K. Dong, *Crystals*, 2018, **8**, 77; (*b*) P. Wang and L. Zhao, *Synth. React. Inorg., Met.-Org., Nano-Met. Chem.*, 2016, **46**, 1095–1101; (*c*) L. Zhao, L. Wang, Y. X. Sun, W. K. Dong, X. L. Tang and X. H. Gao, *Synth. React. Inorg., Met.-Org., Nano-Met. Chem.*, 2012, **42**, 1303–1308.

17 P. Seth, S. Ghosh, A. Figuerola and A. Ghosh, *Dalton Trans.*, 2013, **43**, 990–998.

18 (*a*) X. Y. Dong, Q. Zhao, L. W. Zhang, H. R. Mu, H. Zhang and W. K. Dong, *Molecules*, 2018, **23**, 1006; (*b*) Q. Zhao, X. X. An, L. Z. Liu and W. K. Dong, *Inorg. Chim. Acta*, 2019, **490**, 6–15.

19 (*a*) X. X. An, Q. Zhao, H. R. Mu and W. K. Dong, *Crystals*, 2019, **9**, 101; (*b*) L. Wang, X. Y. Li, Q. Zhao, L. H. Li and W. K. Dong, *RSC Adv.*, 2017, **7**, 48730–48737; (*c*) H. J. Zhang, J. Chang, H. R. Jia and Y. X. Sun, *Chin. J. Inorg. Chem.*, 2018, **34**, 2261–2270.

20 (*a*) Y. J. Dong, X. Y. Dong, W. K. Dong, Y. Zhang and L. S. Zhang, *Polyhedron*, 2017, **123**, 305–315; (*b*) L. W. Zhang, L. Z. Liu, F. Wang and W. K. Dong, *Molecules*, 2018, **23**, 1141.

21 B. Yu, C. Y. Li, Y. X. Sun, H. R. Jia, J. Q. Guo and J. Li, *Spectrochim. Acta, Part A*, 2017, **184**, 249–254.

22 (*a*) G. Li, J. Hao, L. Z. Liu, W. M. Zhou and W. K. Dong, *Crystals*, 2017, **7**, 217; (*b*) Y. Zhang, L. Z. Liu, Y. D. Peng, N. Li and W. K. Dong, *Transition Met. Chem.*, 2019, **44**, 627–639.

23 (*a*) Q. P. Kang, X. Y. Li, L. Wang, Y. Zhang and W. K. Dong, *Appl. Organomet. Chem.*, 2019, **32**, e5013; (*b*) Y. X. Sun, Y. Y. Zhao, C. Y. Li, B. Yu, J. Q. Guo and J. Li, *Chin. J. Inorg. Chem.*, 2016, **32**, 913–920.

24 (*a*) X. Y. Li, Q. P. Kang, C. Liu, Y. Zhang and W. K. Dong, *New J. Chem.*, 2019, **43**, 4605–4619; (*b*) H. R. Jia, J. Chang, H. J. Zhang, J. Li and Y. X. Sun, *Crystals*, 2018, **8**, 272; (*c*) J. Li, H. J. Zhang, J. Chang, H. R. Jia, Y. X. Sun and Y. Q. Huang, *Crystals*, 2018, **8**, 176; (*d*) Q. P. Kang, X. Y. Li, Z. L. Wei, Y. Zhang and W. K. Dong, *Polyhedron*, 2019, **165**, 38–50.

25 W. K. Dong, J. C. Ma, L. C. Zhu and Y. Zhang, *Cryst. Growth Des.*, 2016, **16**, 6903–6914.